Opioid use does not limit potent low-dose HIV-1 latency reversal agent boosting

Tyler Lilie[1]†, Jennifer Bouzy[1]†, Archana Asundi[2], Jessica Taylor[2,3], Samantha Roche[2], Alex Olson[2], Kendyll Coxen[1], Heather Corry[1], Hannah Jordan[1], Kiera Clayton[4], Nina Lin[2]‡, Athe Tsibris[1,5]‡*

† These authors contributed equally to this work

‡ These authors contributed equally to this work

Affiliations:

[1]Brigham and Women's Hospital, Boston, MA, USA.

[2]Department of Medicine, Boston University School of Medicine & Boston Medical Center, Boston, MA USA.

[3]Grayken Center for Addiction, Boston Medical Center, Boston, MA USA.

[4]Department of Pathology, University of Massachusetts T.H. Chan School of Medicine, Worcester, MA, USA.

[5]Harvard Medical School, Boston, MA, USA.

*Corresponding author: atsibris@bwh.harvard.edu

Abstract

The combined effects of the HIV-1 and opioid epidemics on virus reservoir dynamics are less well characterized. To assess the impact of opioid use on HIV-1 latency reversal, we studied forty-seven suppressed participants with HIV-1 and observed that lower concentrations of combination latency reversal agents (LRA) led to synergistic virus reactivation *ex vivo*, regardless of opioid use. The use of a Smac mimetic or low-dose protein kinase C agonist, compounds that did not reverse latency alone, in combination with low-dose histone deacetylase inhibitors generated significantly more HIV-1 transcription than phorbol 12-myristate 13-acetate (PMA) with ionomycin, the maximal known HIV-1 reactivator. This LRA boosting did not differ by sex or race and associated with greater histone acetylation in $CD4^+$ T cells and modulation of T cell phenotype. Virion production and the frequency of multiply spliced HIV-1 transcripts did not increase, suggesting a post-transcriptional block still limits potent HIV-1 LRA boosting.

45 **Introduction**

46 HIV-1 proviral DNA remains integrated in $CD4^+$ T cells during suppressive antiretroviral
47 therapy (ART) and is a barrier to cure. This virus reservoir is seeded within days of infection
48 before symptoms develop[1,2], persists[3-5], decays slowly[6], and can be maintained indefinitely[7,8].
49 The best approach to pursue HIV eradication remains uncertain. One strategy aims to
50 pharmacologically reactivate latent HIV transcription in the setting of suppressive ART, induce
51 virus protein production in infected cells, and then clear the reservoir, defined as cells that
52 contain provirus capable of generating infectious virions, through immune-mediated
53 mechanisms[9-11]. HIV-1 latency reversal agents (LRA) have advanced into clinical trials as
54 monotherapy but with modest results; transient increases in virus mRNA production may be
55 observed with some LRA but does not result in a decrease in reservoir size[12-22]. HIV-1 latency
56 may be characterized by transcriptional blocks that cannot be overcome by single LRA[23-26].

57 To address these limitations, novel classes and combinations of LRA have been studied[27].
58 Epigenetic LRA such as histone deacetylase inhibitors, when combined with protein kinase C
59 agonists or second mitochondria-derived activator of caspase (Smac) mimetics, have been
60 reported under some conditions to synergistically increase HIV-1 transcription in $CD4^+$ T cells
61 isolated from treated suppressed participants with HIV, although the precise mechanism for this
62 synergy is unknown[28-32]. The absolute amount of HIV-1 latency reversal, defined most
63 commonly as induced levels of HIV-1 cell-associated RNA (caRNA), reported with combination
64 LRA is significantly less than that observed with the maximal HIV-1 reactivator, phorbol 12-
65 myristate 13-acetate (PMA) and ionomycin. The effects of combination LRA on multiple
66 splicing of HIV-1 RNA has been less well studied. A trade-off may exist between maximum
67 synergy and maximum efficacy in combination LRA approaches[33].

68 People with HIV may be exposed to opioids, whether prescribed for chronic pain[34],
69 prescribed for opioid use disorder[35], or injected as heroin[36] and have nearly double the risk of
70 overdose compared to uninfected people who use opioids[37]. The pharmacology of opioids
71 associated with substance use disorders may differ from opioid medications used to treat chronic
72 pain. The μ opioid agonists, e.g. heroin, fentanyl, and methadone, can block IL-2 mRNA and
73 protein production in activated T cells through inhibition of AP-1, NFAT, and NF-κB activation,
74 transcription factors known to be positive regulators of HIV transcription initiation [38-40]. The
75 effects of buprenorphine, a partial μ opioid agonist and κ and δ opioid antagonist used in the
76 treatment of opioid use disorder, on HIV-1 latency and its reversal have not been explored. A
77 recent finding suggested that people with HIV who use opioids may have diminished responses
78 to latency reversal[41]; LRA efficacy in this burgeoning patient population is understudied.

79 To investigate the mechanisms that control HIV-1 latency reversal during opioid use, we
80 enrolled a cohort of thirty-six treated, virologically suppressed participants with HIV. We tested
81 LRA combinations at concentrations lower than those typically assessed and identified the
82 phenomenon of LRA boosting: synergistic HIV-1 transcriptional reactivation with small
83 molecules that do not reverse latency as single agents. We corroborated these findings in an
84 additional eleven participants from a separate cohort without opioid use and identified key
85 associations between potent LRA boosting, increases in histone acetylation, modulation of T cell
86 phenotype and function, and downstream blocks in HIV-1 virion production. Importantly, we
87 find that opioid use did not limit the magnitude or mechanisms of LRA boosting.

88

89

90

91 **Results**

92 **Opioid use does not affect HIV-1 reservoir size**

93 We enrolled a cohort from a single academic center of thirty-six treated suppressed participants
94 with HIV who used, or did not use, opioids in a 2:1 ratio. Participants had a median age of 59
95 years, included one-third women, and were approximately 30% white (**Table 1**). The average
96 duration of antiretroviral therapy was 12 years with a median duration of undetectable plasma
97 HIV-1 RNA levels of over six years. Participant characteristics were further defined by type of
98 opioid use (**Suppl. Table 1**) and validated by urine toxicology and self-reported substance use
99 questionnaires (**Suppl. Fig. 1**). This cohort comprised participants who actively injected opioids
100 (n=4), used methadone (n=4) or suboxone (n=12) as medication for opioid use disorder, or took
101 opioids for chronic pain (n=4). Amphetamine and barbiturate use was not detected. All active
102 injection opioid users had confirmatory urine toxicology screens positive for fentanyl (n=2 of 4,
103 range 62 - >500 ng/mL) and/or norfentanyl (n=4 of 4 participants, range 46 - >500 ng/mL) and
104 reported a median of 6 days of injection opioid use in the preceding 30 days (IQR 4-16 days)
105 with a median of 7 days since the most recent use (IQR 4-14 days). All participants in the
106 methadone, buprenorphine, and prescription opioid subgroups had urine toxicology positive for
107 that substance.

108 To assess markers of HIV-1 persistence, we quantified total HIV-1 DNA and caRNA in
109 PBMC and evaluated intact proviral reservoir size. Total HIV-1 DNA levels were similar
110 between opioid and non-opioid groups, 2.36 vs 2.38 $\log_{10}$ copies/10^6 PBMC, respectively, as
111 were HIV-1 caRNA levels, 2.45 vs 2.52 $\log_{10}$ copies/10^6 PBMC (**Fig. 1a**). Levels of intact
112 provirus DNA were also similar between groups, 2.00 vs 1.82 $\log_{10}$ copies/10^6 PBMC. To better
113 define the intact proviral DNA reservoir, we characterized 5' and 3' HIV-1 deletions across

114 cohorts and opioid use subgroups (**Fig. 1b-c**). Similar proportions of intact 5' and 3' genetic
115 regions were observed, irrespective of opioid use. The ratios of proviruses containing an intact 5'
116 region and a defective (hypermutated) or deleted 3' region in HIV-1 *env* were statistically
117 similar. An exploratory analysis demonstrated a greater proportion of total genomes were intact
118 in active opioid users (**Fig. 1d**).

119

120 **LRA boosting markedly increases HIV-1 transcription**

121 To determine the effects of opioid use on HIV-1 latency reversal *ex vivo*, we isolated
122 PBMC from all OPHION participants and tested a panel of ten LRA conditions (**Fig. 2**). The
123 histone deacetylase inhibitors (HDACi) romidepsin (RMD) and panobinostat (PNB) were used at
124 the lowest concentrations most commonly reported in the literature and the protein kinase C
125 agonist bryostatin was tested at 1nM, one-tenth the most commonly reported concentration. In
126 single LRA conditions, we observed a 2.7-fold activation of HIV-1 caRNA transcription, relative
127 to an untreated DMSO-containing control, with αCD3/αCD28 beads (95% CI [2.2, 3.2]), a T cell
128 receptor (TCR) agonist (**Fig. 2a**). Greater reactivation was observed with RMD (3.8-fold
129 increase, 95% CI [3.2, 4.3]) when compared to PNB (2.6-fold increase, 95% CI [2.2, 3.0]). Low-
130 dose bryostatin minimally increased unspliced HIV-1 caRNA levels (1.2-fold increase, 95% CI
131 [1.1, 1.4]), but the Smac mimetic AZD5582, at a standard concentration[42], did not (0.9-fold
132 increase, 95% CI [0.8, 1.1]).

133 We next assessed LRA in combination. Incubation of PBMC with HDACi and either
134 AZD5582 (AZD) or low-dose bryostatin potentiated HIV-1 latency reversal. AZD in
135 combination with PNB or RMD increased HIV-1 caRNA levels 8.1-fold (95% CI [6.5, 9.2]) and
136 9.1-fold (95% CI [7.4, 10.8]), respectively. Low-dose bryostatin with PNB increased HIV-1

137 caRNA 10.6-fold (95% CI [8.9, 12.2]), whereas the greatest fold-induction of HIV-1 caRNA was
138 observed with the combination of low-dose bryostatin and RMD (13.2-fold, 95% CI [11.2,
139 15.2]). Statistically greater HIV-1 RNA induction was observed with the LRA boosting
140 combinations relative to HDACi monotherapy and TCR agonism, when corrected for multiple
141 comparisons. We compared LRA response as a function of opioid use (**Fig. 2b**), sex (**Fig. 2c**),
142 race (**Fig. 2d**), and ethnicity (**Suppl. Fig. 2**) and observed no statistically significant differences
143 in the fold-changes of HIV-1 caRNA induction across these groups. In an exploratory analysis,
144 the fold-change in HIV-1 caRNA varied by opioid use subgroup in response to T cell receptor
145 agonism (**Fig. 2e**). Statistically significantly greater reactivation was observed in the suboxone
146 sub-group when compared to active injection opioid users, the group with the smallest fold-
147 change in αCD3/αCD28 bead-induced HIV-1 caRNA levels.

148

149 **LRA boosting modulates T cell activation and cytokine production**

150 To understand whether LRA exposure activates $CD4^+$ T cells, we assessed the
151 upregulation of surface activation-induced markers (AIM) [43]. We leveraged dual-marker AIM
152 assays (**Suppl. Fig. 3, Fig. 3a**), originally developed to detect T cell antigen responsiveness, to
153 quantify cellular activation that occurs with LRA exposure, outside the context of peptide-
154 specific recognition. Using TCR agonism as a positive control, responses were detected in 49%
155 (95% CI [45, 54]), 32% (95% CI [28, 35]), and 42% (95% CI [36, 47]) of $CD4^+$ T cells in the
156 OX40/PDL1, OX40/CD25, and CD69/CD40L AIM assays, respectively (**Fig. 3b**). Low-dose
157 bryostatin significantly upregulated surface expression to more modest levels in all three AIM
158 assays, relative to an untreated control condition. Bryostatin induced OX40/PDL1 surface
159 expression in 5.2% of $CD4^+$ T cells (95% CI [3,4, 7.0]), levels of induction that did not

160 significantly change when used in combination with RMD (5.4%, 95% CI [3.3, 7.4]) or PNB
161 (3.5%, 95% CI [2.1, 5.0]). Bryostatin monotherapy induced expression in 6.9% (95% CI [5.6,
162 8.3]) and 2.6% (95% CI [2.0, 3.2]) of CD4s in the OX40/CD25 and CD69/CD40L AIM assays,
163 respectively. In these two assays, the combination of RMD or PNB with low-dose bryostatin
164 reduced activation-induced markers, relative to bryostatin alone, in some cases to undetectable
165 levels; these findings did not differ by opioid use. The remainder of the LRA panel and their
166 combinations did not upregulate surface expression in any AIM assay (**Suppl. Fig. 4a-c)**.

167 We observed a more pronounced upregulation in isolated CD69 expression, an early
168 activation marker, in response to LRA (**Fig. 3c**). Approximately 0.5% (95% CI [0.4, 0.7]) of
169 untreated $CD4^+$ T cells expressed CD69 after 18 hours in culture. The proportion of cells
170 expressing surface CD69 significantly increased to similar levels with TCR agonism (68.5%,
171 95% CI [63.1, 73.9]) and low-dose bryostatin (72.9%, 95% CI [69.2, 76.5]). Whereas AZD5582
172 (1.0%, 95% CI [0.7, 1.2]), RMD (4.7%, 95% CI [3.1, 6.3]), and PNB (5.4%, 95% CI [3.8, 7.0])
173 modestly increased CD69 levels, combinations of these small molecules led to synergistic
174 effects. Significantly greater induction of CD69 expression was observed when RMD or PNB
175 was combined with bryostatin or AZD5582; a bryostatin combination induced more CD69 than
176 an HDACi plus AZD5582. CD69 levels were statistically similar when comparing TCR
177 agonism, bryostatin alone, and bryostatin in combination with either HDACi (**Suppl. Fig. 4d**).

178 To further assess LRA effects on T cell activation, we stained $CD4^+$ and $CD8^+$ T cells for
179 intracellular cytokine production (**Fig. 3d-e**). We observed a cytokine production hierarchy in
180 CD4s, where TNF-α > IL-2 > IFN-γ, and in CD8s, where TNF-α > IFN-γ > IL-2. In response to
181 TCR agonism, significantly more $CD4^+$ T cells (CD4s) produce TNF-α (30.4%, 95% CI [27.5,
182 33.4]) than IL-2 (14.3%, 95% CI [12.5, 16.1]) or IFN-γ (6.0%, 95% CI [4.9, 7.1]), and

183 significantly more IL-2 than IFN-γ (**Suppl. Fig. 4e**). We identified a different hierarchy in $CD8^+$
184 T cells (CD8s), where the proportion of cells producing TNF-α remained greatest (17.5%, 95%
185 CI [13.9, 21.1]) but significantly more IFN-γ (9.0%, 95% CI [7.1, 10.9]) was produced than IL-2
186 (4.3%, 95% CI [2.8, 5.9]). Whereas HDACi monotherapy did not increase the proportion of
187 CD4s or CD8s producing cytokines compared to an untreated control, low-dose bryostatin alone
188 or in combination with HDACi significantly increased production of TNF-α and, to a smaller
189 magnitude, IFN-γ in CD4s. Significantly more CD4s produced TNF-α than IFN-γ in response to
190 RMD + bryostatin (4.5%, 95% CI [3.5, 5.6] versus 1.3%, 95% CI [0.9, 1.7]) and PNB +
191 bryostatin (4.2%, 95% CI [3.4, 5.0] versus 1.7%, 95% CI [1.0, 2.4]). In CD8s, low-dose
192 bryostatin significantly increased production of TNF-α (2.8%, 95% CI [1.9, 3.8]) and IFN-γ
193 (1.5%, 95% CI [0.9, 2.0]). The proportions of CD8s that produced TNF-α and IFN-γ when
194 exposed to the combinations of RMD + bryostatin (3.4%, 95% CI [2.5, 4.4] versus 4.7%, 95% CI
195 [2.8, 6.6]) and PNB + bryostatin (4.1%, 95% CI [2.9, 5.3] versus 4.6%, 95% CI [3.0, 6.3]) were
196 similar. IL-2 production did not increase above 0.1% of CD4s or CD8s for any LRA, or
197 combination, we tested. Cytokine production did not differ by opioid use (**Suppl. Fig. 5**).

198

199 **LRA boosting increases histone acetylation**

200 To investigate the mechanism(s) of LRA boosting, we next assessed histone acetylation.
201 The proportions of acetylated histone $H3^+$ live CD4s were similar between untreated cells
202 (19.7%, 95% CI [16.9, 22.4]) and cells exposed to RMD (21.8%, 95% CI [19.4, 24.3]), PNB
203 (21.7%, 95% CI [19.3, 24.2]), or AZD (19.8%, 95% CI [17.1, 22.6]) and significantly increased
204 after single-LRA exposure to αCD3/αCD28 beads (35.5%, 95% CI [32.7, 38.4]) and low-dose
205 bryostatin (29.2%, 95% CI [25.7, 32.6]) (**Fig. 4a**). Low-dose bryostatin in combination with

206 either RMD (36.8%, 95% CI [32.1, 43.2]) or PNB (37.5%, 95% CI [31.8, 43.2]) significantly
207 increased the proportions of CD4s contained acetylated histone H3. Interestingly, statistically
208 significant increases in acetylated histone $H3^+$ live CD4s were also observed when combining
209 LRA which individually did not affect acetylation, specifically RMD + AZD (30.0%, 95% CI
210 [26.9, 33.1]) and PNB + AZD (29.8%, 95% CI [26.5, 33.0]). These results did not differ by
211 opioid use (**Suppl. Fig 6a**).

212 Levels of acetylated histone H3, measured by median fluorescence intensity (MFI), were
213 similar in untreated live CD4s and in cells cultured with αCD3/αCD28 beads, low-dose
214 bryostatin, or AZD (**Fig. 4b**). Significant 3.4-fold and 3.3-fold increases in acetyl histone MFI
215 were observed for RMD (21482, 95% CI [19014, 23951]) and PNB (21070, 95% CI [18727,
216 23413]), respectively. AZD in combination with RMD or PNB further increased MFI by 6.1-
217 fold and 5.7-fold, respectively. Absolute increases in MFI were observed for low-dose bryostatin
218 in combination with RMD (25498, 95% CI [22772, 28225]) or PNB (27651, 95% CI [24729,
219 30573]) but did not retain significance after correction for multiple comparisons. These results
220 did not differ by opioid use (**Suppl. Fig 6b**). We observed no association between acetylated
221 histone H3 MFI and fold-change in HIV-1 RNA levels for HDACi monotherapy or for HDACi
222 in combination with AZD (**Fig 4c-d**). A statistically significant weak association between the
223 proportion of acetyl histone $H3^+$ CD4s and fold-change in HIV-1 RNA levels was detected for
224 HDACi in combination with bryostatin (**Fig 4e**).

225

226 **LRA boosting does not consistently induce virion production**

227 To extend our analyses from the OPHION cohort, we studied an additional eleven
228 participants with HIV who did not use opioids, enrolled in the HEAL cohort (**Suppl. Table 2**).

229 We compared LRA boosting responses to the most potent known HIV-1 LRA, PMA in
230 combination with ionomycin (PMA-iono). Significant fold-change increases in HIV-1
231 transcription were observed with combinations of low-dose bryostatin with RMD (8.3-fold, 95%
232 CI [7.2, 9.5]) or PNB (8.0-fold, 95% CI [6.9, 9.0]), when compared to RMD alone (3.4-fold,
233 95% CI [2.6, 4.2]), PNB alone (3.1-fold, 95% CI [2.6, 3.6]), or PMA-iono (1.6-fold, 95% CI
234 [1.4, 1.9]) (**Fig. 5a**). In separate experiments, we did not observe statistically greater HIV-1
235 transcription with an HDACi in combination with AZD, relative to PMA-iono, in contrast to the
236 results from the larger OPHION cohort (**Fig 5b**). No significant increases in HIV-1 transcription
237 were observed in PBMC experiments with low-dose bryostatin (1.0-fold, 95% CI 0.9 – 1.1) or
238 AZD (1.2-fold, 95% CI 0.6 – 1.9). Similar magnitudes of HIV-1 transcriptional reactivation were
239 seen with HDACi monotherapy, low-dose bryostatin, and AZD monotherapy across the
240 OPHION and HEAL cohorts we studied. We evaluated human reference gene transcription
241 during LRA treatment and observed decreases with HDACi exposure, increases with PMA-iono,
242 and variable changes with bryostatin (**Suppl. Fig. 7**).[44,45]

243 To assess the magnitude of HIV-1 latency reversal as a function of cell type, we next
244 performed parallel experiments in PBMC and total $CD4^+$ T cells (**Fig. 5c**). Levels of HIV-1
245 caRNA were, on average, 4.3-fold higher (range 3.2 – 6.0) across experimental conditions
246 performed in $CD4^+$ T cells, when compared to PBMC, and varied by 1.6 $\log_{10}$ (PBMC) and 1.8
247 $\log_{10}$ (CD4) across participant samples in the absence of LRA. To control for absolute caRNA
248 differences, we determined fold-changes in LRA response and observed statistically significant
249 increases in HIV-1 caRNA with low-dose bryostatin in combination with RMD or PNB, when
250 compared to PMA-iono, in both PBMC and CD4s (**Fig. 5d**). To explore the variance in LRA
251 response, we compiled per-participant biological replicate measurements (**Suppl. Fig. 8a**).

252 Supernatant HIV-1 RNA levels increased after 24hr incubation of PBMC with PMA-iono (19
253 copies/mL, 95% CI [10, 32]) and the combinations of RMD plus bryostatin (27 copies/mL, 95%
254 CI [11, 34]) or AZD (31 copies/mL, 95% CI [14, 43]), and PNB plus bryostatin (35 copies/mL,
255 95% CI [19, 60]) or AZD (12 copies/mL, 95% CI [8.1, 26]), when compared to untreated PBMC
256 (3.0 copies/mL, 95% CI [2.2, 6.9]), but these results were not statistically significant after
257 correction for multiple comparisons (**Fig. 5e**). This virion production response was biphasic. For
258 each LRA condition, PBMC samples from at least 5 of 10 participants showed no increases in
259 HIV-1 RNA levels over control; these were most commonly the same participants. Additionally,
260 no significant increases in LRA-induced virion production in $CD4^+$ T cell cultures were
261 observed. Notably, greater virion production in untreated CD4s and greater absolute magnitudes
262 of supernatant viremia in LRA treated CD4s were noted, relative to PBMC, but were again
263 driven by increases from a subset of participants. To investigate the nature of this post-
264 transcriptional block more precisely, we quantified the frequency of CD4s with inducible
265 multiply spliced HIV-1 RNA transcripts (**Fig. 5f**) [46]. No significant increases in HIV-1 *tat*/*rev*
266 transcripts were observed with RMD in combination with bryostatin at either 1nM or 10nM
267 concentrations. In a post-hoc analysis, we combined datasets from OPHION and HEAL
268 participants, including LRA conditions common to both sets of experiments, and observed
269 statistically significant increases in HIV-1 unspliced RNA transcription with all LRA boosting
270 combinations (**Fig. 5g**). The variance in LRA responseincreased as the magnitude of fold change
271 in HIV-1 caRNA increased (**Suppl. Fig 8b**).

272

273

274

275 **Discussion**

276 Opioid use is complex and can be accompanied by comorbidities, such as immune
277 activation with injection drug use [47,48], that may impact the HIV-1 reservoir and its persistence
278 [45,49-52]. Here, we found no effects of opioid use by indication, type, or pharmacology on markers
279 of HIV-1 persistence. In the setting of persistently suppressed viremia, opioid use was less likely
280 to modulate virus reservoir size. While our OPHION study participants were older than opioid
281 users experiencing the greatest number of overdose deaths [53], they do reflect an age more typical
282 for patients with HIV who engage in research locally. Overall, participants were matched on the
283 duration of ART and the duration of virus suppression, key variables that have been associated
284 with HIV-1 reservoir size, [54] and our urine toxicology results were consistent with the
285 participants' ascribed opioid use group. We found that opioid use generally did not impact LRA
286 responsiveness, in contrast to a recent smaller study [41]. Our relatively large sample size allowed
287 us to determine that this potency was less likely to be affected by sex, race, or ethnicity.

288 We used these samples to identify and characterize the phenomenon of LRA boosting:
289 improving the potency of HDACi beyond that of PMA-ionomycin by combining with a 2nd drug
290 that does not, by itself, re-activate HIV-1 transcription. This boosting occurred at lower LRA
291 concentrations, here at least half the RMD and 1/10th the bryostatin concentrations used in prior
292 combination studies [28-31]. The specific synergistic latency reversal effects of low-dose bryostatin
293 and romidepsin was previously identified in samples from four participants with HIV [28]. Here we
294 confirm those findings in a larger sample size and extend the observation to HDACi more
295 generally. While AZD5582 monotherapy induced virus transcription in tissues from animal
296 models, we observed no HIV-1 latency reversal, at an identical dose, in PBMC isolated from the
297 47 participants we tested [42]. We observed greater *ex vivo* LRA efficacy of HDACi monotherapy,

298 relative to AZD5582. In this regard, our findings agree with a recent study that assessed a higher
299 AZD5582 concentration, although this study did not identify HDACi-AZD synergy, relative to
300 HDACi monotherapy, using higher LRA concentrations [32]. Interestingly, the fold-change in
301 HIV-1 RNA levels that we observed with PMA-ionomycin were orders of magnitude lower than
302 some prior studies [28,32]. Here, we calculated levels of HIV-1 caRNA copy number in response to
303 LRA on a per-cell basis, rather than the induction of HIV-1 transcripts on a weight basis, per μg
304 of RNA. These differences did not appear to be a function of the cell type used for latency
305 reversal, PBMC versus total $CD4^+$ T cells, and it remains unclear if assay technicalities or
306 quantification methodology may contribute.

307 The use of two HDACi in our panel of ten LRA conditions increased the generalizability
308 of the findings we observed with this drug class. Similar magnitudes of boosting were observed
309 with RMD and PNB and suggests that class I histone deacetylase inhibition may be more
310 relevant to this phenomenon [55]. LRA boosting correlated with increased histone H3 acetylation
311 in $CD4^+$ T cells but AZD-associated boosting did not recruit additional CD4s with acetylated
312 histone H3. HDACi monotherapy also did not increase the proportions of acetylated histone H3-
313 positive CD4s and the amount of acetylated histone H3 per cell did not meaningfully correlate
314 with the induction of HIV-1 transcription. It remains unclear if histone acetylation is correlative
315 or causative to virus reactivation. In the context of cellular genes, histone acetylation is not an
316 immediate driver of the transcriptional changes observed with HDACi [56]. Similar magnitudes of
317 HIV-1 reactivation were observed with low-dose bryostatin- and AZD5582-mediated HDACi
318 boosting and could share common mechanisms. Bryostatin and AZD5582 can activate canonical
319 and non-canonical NF-κB pathways, respectively, and the overlap in signaling with LRA
320 boosting requires further definition.

321 LRA boosting, and their individual components, can have off-target effects. Whereas
322 CD69 surface expression has been proposed as a biomarker of latency reversal potency in the
323 context of PKC agonists, we found no correlation between CD69 upregulation and the magnitude
324 of latency reversal [57]. Low-dose bryostatin was sufficient to increase surface activation-induced
325 markers and increase cytokine production in $CD4^+$ and $CD8^+$ T cells, albeit to relatively low
326 levels, either alone or in combination with HDACi. Our results confirm and extend previous
327 findings on the effects of combination LRA on T lymphocytes [58]. In contrast, LRA boosting
328 with AZD5582 resulted in relatively lower surface levels of CD69 and no induction of surface
329 activation markers or cytokine production in T cells. An LRA boosting approach that minimizes
330 immune modulatory effects may be more appealing as an investigational intervention.

331 The variance in HIV-1 LRA responsiveness we document, across participants and
332 replicates, has implications for future studies. Small studies may be limited in their capacity to
333 accurately quantify this variability, which increases with LRA potency. Assessments of LRA
334 activity should prioritize larger sample sizes and more than one biological replicate per
335 participant. We found that normalization of HIV-1 transcription to host gene transcription may
336 introduce additional variability. Despite HIV-1 re-activation that was superior to PMA-
337 ionomycin, multiply spliced HIV-1 transcription and virion production did not increase with
338 LRA boosting. Blocks to HIV-1 splicing are increasingly recognized, and here we extend those
339 findings to novel LRA boosting combinations [23-25,59-61]. Future work must focus on the post-
340 transcriptional mechanisms of HIV-1 RNA processing and inter-patient differences in LRA
341 responsiveness, which facilitate virion production during TCR agonism and treatment with
342 PMA-ionomycin and which may not be active during HIV-1 latency or LRA boosting.

343 Our study has limitations. Prior and current injection opioid use limits the peripheral
344 blood draw volumes we could obtain; this required us to prioritize experiments with a given
345 sample. The statistical significance of LRA boosting with AZD5582-containing regimens was
346 not replicated in our HEAL cohort samples and it is unclear if this relates to the variability in
347 LRA response as sample size decreases or to unrecognized differences between our cohort's
348 participants. Additional mechanisms are likely to explain how LRA boosting increases virus
349 transcription. Bryostatin may exert its HIV-1 latency reversal effects independently of PKC
350 agonism [62].

351 The use of HIV-1 LRA at sub-maximal doses and in combination with small molecules
352 that do not increase virus transcription, *ex vivo*, expands our understanding of how virus latency
353 may be reversed. Follow-on studies should delineate the precise mechanisms required for
354 efficient virus RNA processing and virion production and identify new discovery targets for
355 future development.

356

357 **Acknowledgements**

358 This work is supported by the National Institutes of Health (NIH) R61 DA047038 (NL and AT)
359 and R33 DA047038 (AT) and was facilitated by the Providence/Boston Center for AIDS
360 Research (P30AI042853) and the Harvard University Center for AIDS Research (P30AI060354).
361 The project described was further supported by Clinical Translational Science Award
362 1UL1TR002541-01 to Harvard University and Brigham and Women's Hospital from the
363 National Center for Research Resources. The content is solely the responsibility of the authors
364 and does not necessarily represent the official views of the National Center for Research
365 Resources or the National Institutes of Health.

366 **References**

367 1. Chun, T.W., *et al.* Early establishment of a pool of latently infected, resting CD4(+) T
368 cells during primary HIV-1 infection. *Proceedings of the National Academy of Sciences*
369 *of the United States of America* **95**, 8869-8873 (1998).
370 2. Whitney, J.B., *et al.* Rapid seeding of the viral reservoir prior to SIV viraemia in rhesus
371 monkeys. *Nature* **512**, 74-77 (2014).
372 3. Wong, J.K., *et al.* Recovery of replication-competent HIV despite prolonged suppression
373 of plasma viremia. *Science (New York, N.Y* **278**, 1291-1295 (1997).
374 4. Chun, T.W., *et al.* Presence of an inducible HIV-1 latent reservoir during highly active
375 antiretroviral therapy. *Proceedings of the National Academy of Sciences of the United*
376 *States of America* **94**, 13193-13197 (1997).
377 5. Finzi, D., *et al.* Latent infection of CD4+ T cells provides a mechanism for lifelong
378 persistence of HIV-1, even in patients on effective combination therapy. *Nature medicine*
379 **5**, 512-517 (1999).
380 6. Siliciano, J.D., *et al.* Long-term follow-up studies confirm the stability of the latent
381 reservoir for HIV-1 in resting CD4+ T cells. *Nature medicine* **9**, 727-728 (2003).
382 7. Chomont, N., *et al.* HIV reservoir size and persistence are driven by T cell survival and
383 homeostatic proliferation. *Nature medicine* **15**, 893-900 (2009).
384 8. Mullins, J.I. & Frenkel, L.M. Clonal Expansion of Human Immunodeficiency Virus-
385 Infected Cells and Human Immunodeficiency Virus Persistence During Antiretroviral
386 Therapy. *The Journal of infectious diseases* **215**, S119-S127 (2017).
387 9. Deeks, S.G., *et al.* International AIDS Society global scientific strategy: towards an HIV
388 cure 2016. *Nature medicine* (2016).

389 10. Ferrari, G., Pollara, J., Tomaras, G.D. & Haynes, B.F. Humoral and Innate Antiviral
390 Immunity as Tools to Clear Persistent HIV Infection. *The Journal of infectious diseases*
391 **215**, S152-S159 (2017).
392 11. Riley, J.L. & Montaner, L.J. Cell-Mediated Immunity to Target the Persistent Human
393 Immunodeficiency Virus Reservoir. *The Journal of infectious diseases* **215**, S160-S171
394 (2017).
395 12. McMahon, D.K.*, et al.* A Phase 1/2 Randomized, Placebo-Controlled Trial of
396 Romidespin in Persons With HIV-1 on Suppressive Antiretroviral Therapy. *The Journal*
397 *of infectious diseases* **224**, 648-656 (2021).
398 13. Scully, E.P.*, et al.* Impact of Tamoxifen on Vorinostat-Induced Human
399 Immunodeficiency Virus Expression in Women on Antiretroviral Therapy: AIDS
400 Clinical Trials Group A5366, The MOXIE Trial. *Clin Infect Dis* **75**, 1389-1396 (2022).
401 14. Gutierrez, C.*, et al.* Bryostatin-1 for latent virus reactivation in HIV-infected patients on
402 antiretroviral therapy. *AIDS (London, England)* **30**, 1385-1392 (2016).
403 15. Archin, N.M.*, et al.* HIV-1 expression within resting CD4+ T cells after multiple doses of
404 vorinostat. *The Journal of infectious diseases* **210**, 728-735 (2014).
405 16. Archin, N.M.*, et al.* Administration of vorinostat disrupts HIV-1 latency in patients on
406 antiretroviral therapy. *Nature* **487**, 482-485 (2012).
407 17. Elliott, J.H.*, et al.* Activation of HIV transcription with short-course vorinostat in HIV-
408 infected patients on suppressive antiretroviral therapy. *PLoS pathogens* **10**, e1004473
409 (2014).
410 18. Sogaard, O.S.*, et al.* The Depsipeptide Romidepsin Reverses HIV-1 Latency In Vivo.
411 *PLoS pathogens* **11**, e1005142 (2015).

412 19. Rasmussen, T.A., *et al.* Panobinostat, a histone deacetylase inhibitor, for latent-virus
413 reactivation in HIV-infected patients on suppressive antiretroviral therapy: a phase 1/2,
414 single group, clinical trial. *The lancet. HIV* **1**, e13-21 (2014).
415 20. Routy, J.P., *et al.* Valproic acid in association with highly active antiretroviral therapy for
416 reducing systemic HIV-1 reservoirs: results from a multicentre randomized clinical study.
417 *HIV medicine* **13**, 291-296 (2012).
418 21. Sagot-Lerolle, N., *et al.* Prolonged valproic acid treatment does not reduce the size of
419 latent HIV reservoir. *AIDS (London, England)* **22**, 1125-1129 (2008).
420 22. Archin, N.M., *et al.* Interval dosing with the HDAC inhibitor vorinostat effectively
421 reverses HIV latency. *The Journal of clinical investigation* **127**, 3126-3135 (2017).
422 23. Yukl, S.A., *et al.* HIV latency in isolated patient CD4(+) T cells may be due to blocks in
423 HIV transcriptional elongation, completion, and splicing. *Science translational medicine*
424 **10**(2018).
425 24. Moron-Lopez, S., *et al.* Characterization of the HIV-1 transcription profile after
426 romidepsin administration in ART-suppressed individuals. *AIDS (London, England)* **33**,
427 425-431 (2019).
428 25. Zerbato, J.M., *et al.* Multiply spliced HIV RNA is a predictive measure of virus
429 production ex vivo and in vivo following reversal of HIV latency. *EBioMedicine* **65**,
430 103241 (2021).
431 26. Martin, H.A., *et al.* New Assay Reveals Vast Excess of Defective over Intact HIV-1
432 Transcripts in Antiretroviral Therapy-Suppressed Individuals. *Journal of virology* **96**,
433 e0160522 (2022).

434 27. Rodari, A., Darcis, G. & Van Lint, C.M. The Current Status of Latency Reversing Agents
435 for HIV-1 Remission. *Annu Rev Virol* **8**, 491-514 (2021).
436 28. Laird, G.M.*, et al.* Ex vivo analysis identifies effective HIV-1 latency-reversing drug
437 combinations. *The Journal of clinical investigation* **125**, 1901-1912 (2015).
438 29. Pache, L.*, et al.* BIRC2/cIAP1 Is a Negative Regulator of HIV-1 Transcription and Can
439 Be Targeted by Smac Mimetics to Promote Reversal of Viral Latency. *Cell host &*
440 *microbe* **18**, 345-353 (2015).
441 30. Grau-Exposito, J.*, et al.* Latency reversal agents affect differently the latent reservoir
442 present in distinct CD4+ T subpopulations. *PLoS pathogens* **15**, e1007991 (2019).
443 31. Pardons, M., Fromentin, R., Pagliuzza, A., Routy, J.P. & Chomont, N. Latency-
444 Reversing Agents Induce Differential Responses in Distinct Memory CD4 T Cell Subsets
445 in Individuals on Antiretroviral Therapy. *Cell Rep* **29**, 2783-2795 e2785 (2019).
446 32. Dai, W.*, et al.* Genome-wide CRISPR screens identify combinations of candidate latency
447 reversing agents for targeting the latent HIV-1 reservoir. *Science translational medicine*
448 **14**, eabh3351 (2022).
449 33. Gupta, V. & Dixit, N.M. Trade-off between synergy and efficacy in combinations of
450 HIV-1 latency-reversing agents. *PLoS computational biology* **14**, e1006004 (2018).
451 34. Edelman, E.J.*, et al.* Receipt of opioid analgesics by HIV-infected and uninfected
452 patients. *J Gen Intern Med* **28**, 82-90 (2013).
453 35. Reddon, H.*, et al.* Methadone maintenance therapy decreases the rate of antiretroviral
454 therapy discontinuation among HIV-positive illicit drug users. *AIDS Behav* **18**, 740-746
455 (2014).

456 36. Tavitian-Exley, I., Vickerman, P., Bastos, F.I. & Boily, M.C. Influence of different drugs
457 on HIV risk in people who inject: systematic review and meta-analysis. *Addiction* **110**,
458 572-584 (2015).
459 37. Green, T.C., McGowan, S.K., Yokell, M.A., Pouget, E.R. & Rich, J.D. HIV infection and
460 risk of overdose: a systematic review and meta-analysis. *AIDS (London, England)* **26**,
461 403-417 (2012).
462 38. Borner, C., Kraus, J., Bedini, A., Schraven, B. & Hollt, V. T-cell receptor/CD28-
463 mediated activation of human T lymphocytes induces expression of functional mu-opioid
464 receptors. *Mol Pharmacol* **74**, 496-504 (2008).
465 39. Borner, C.*, et al.* Mechanisms of opioid-mediated inhibition of human T cell receptor
466 signaling. *J Immunol* **183**, 882-889 (2009).
467 40. Mbonye, U. & Karn, J. Transcriptional control of HIV latency: Cellular signaling
468 pathways, epigenetics, happenstance and the hope for a cure. *Virology* (2014).
469 41. Basukala, B.*, et al.* Virally Suppressed People Living with HIV Who Use Opioids Have
470 Diminished Latency Reversal. *Viruses* **15**(2023).
471 42. Nixon, C.C.*, et al.* Systemic HIV and SIV latency reversal via non-canonical NF-kappaB
472 signalling in vivo. *Nature* **578**, 160-165 (2020).
473 43. Reiss, S.*, et al.* Comparative analysis of activation induced marker (AIM) assays for
474 sensitive identification of antigen-specific CD4 T cells. *PLoS ONE* **12**, e0186998 (2017).
475 44. Ceriani, C.*, et al.* Defining stable reference genes in HIV latency reversal experiments.
476 *Journal of virology* **95**(2021).

477 45. Gandhi, R.T., *et al.* Levels of HIV-1 persistence on antiretroviral therapy are not
478 associated with markers of inflammation or activation. *PLoS pathogens* **13**, e1006285
479 (2017).
480 46. Procopio, F.A., *et al.* A Novel Assay to Measure the Magnitude of the Inducible Viral
481 Reservoir in HIV-infected Individuals. *EBioMedicine* **2**, 874-883 (2015).
482 47. Mehandru, S., *et al.* Behavioural, Mucosal and Systemic Immune Parameters in HIV-
483 infected and Uninfected Injection Drug Users. *J Addict Res Ther* **6**, 1-8 (2015).
484 48. Deren, S., Cleland, C.M., Lee, H., Mehandru, S. & Markowitz, M. Brief Report: The
485 Relationship Between Injection Drug Use Risk Behaviors and Markers of Immune
486 Activation. *Journal of acquired immune deficiency syndromes (1999)* **75**, e8-e12 (2017).
487 49. Khoury, G., *et al.* Human Immunodeficiency Virus Persistence and T-Cell Activation in
488 Blood, Rectal, and Lymph Node Tissue in Human Immunodeficiency Virus-Infected
489 Individuals Receiving Suppressive Antiretroviral Therapy. *The Journal of infectious*
490 *diseases* **215**, 911-919 (2017).
491 50. Massanella, M., Fromentin, R. & Chomont, N. Residual inflammation and viral
492 reservoirs: alliance against an HIV cure. *Current opinion in HIV and AIDS* **11**, 234-241
493 (2016).
494 51. Ruggiero, A., *et al.* During Stably Suppressive Antiretroviral Therapy Integrated HIV-1
495 DNA Load in Peripheral Blood is Associated with the Frequency of CD8 Cells
496 Expressing HLA-DR/DP/DQ. *EBioMedicine* **2**, 1153-1159 (2015).
497 52. Cockerham, L.R., *et al.* CD4+ and CD8+ T cell activation are associated with HIV DNA
498 in resting CD4+ T cells. *PLoS ONE* **9**, e110731 (2014).

499 53. Spencer, M.R., Minino, A.M. & Warner, M. Drug Overdose Deaths in the United States,
500 2001-2021. *NCHS Data Brief*, 1-8 (2022).
501 54. Bachmann, N.*, et al.* Determinants of HIV-1 reservoir size and long-term dynamics
502 during suppressive ART. *Nat Commun* **10**, 3193 (2019).
503 55. Milazzo, G.*, et al.* Histone Deacetylases (HDACs): Evolution, Specificity, Role in
504 Transcriptional Complexes, and Pharmacological Actionability. *Genes (Basel)* **11**(2020).
505 56. Halsall, J.A., Turan, N., Wiersma, M. & Turner, B.M. Cells adapt to the epigenomic
506 disruption caused by histone deacetylase inhibitors through a coordinated, chromatin-
507 mediated transcriptional response. *Epigenetics Chromatin* **8**, 29 (2015).
508 57. Marsden, M.D.*, et al.* In vivo activation of latent HIV with a synthetic bryostatin analog
509 effects both latent cell "kick" and "kill" in strategy for virus eradication. *PLoS pathogens*
510 **13**, e1006575 (2017).
511 58. Walker-Sperling, V.E., Pohlmeyer, C.W., Tarwater, P.M. & Blankson, J.N. The Effect of
512 Latency Reversal Agents on Primary CD8+ T Cells: Implications for Shock and Kill
513 Strategies for Human Immunodeficiency Virus Eradication. *EBioMedicine* **8**, 217-229
514 (2016).
515 59. Wedrychowski, A.*, et al.* Transcriptomic Signatures of Human Immunodeficiency Virus
516 Post-Treatment Control. *Journal of virology* **97**, e0125422 (2023).
517 60. Moron-Lopez, S.*, et al.* Human splice factors contribute to latent HIV infection in
518 primary cell models and blood CD4+ T cells from ART-treated individuals. *PLoS*
519 *pathogens* **16**, e1009060 (2020).

520 61. Mota, T.M., *et al.* Integrated Assessment of Viral Transcription, Antigen Presentation,
521 and CD8(+) T Cell Function Reveals Multiple Limitations of Class I-Selective Histone
522 Deacetylase Inhibitors during HIV-1 Latency Reversal. *Journal of virology* **94**(2020).
523 62. Mbonye, U., Leskov, K., Shukla, M., Valadkhan, S. & Karn, J. Biogenesis of P-TEFb in
524 CD4+ T cells to reverse HIV latency is mediated by protein kinase C (PKC)-independent
525 signaling pathways. *PLoS pathogens* **17**, e1009581 (2021).
526 63. McLellan, A.T., *et al.* The Fifth Edition of the Addiction Severity Index. *J Subst Abuse*
527 *Treat* **9**, 199-213 (1992).
528 64. Institute of Behavioral Research. Texas Christian University Drug Screen 5. Fort Worth:
529 Texas Christian University, Institute of Behavioral Research (2020)
530 (https://ibr.tcu.edu/forms/tcu-drug-screen/).
531 65. Malnati, M.S., *et al.* A universal real-time PCR assay for the quantification of group-M
532 HIV-1 proviral load. *Nature protocols* **3**, 1240-1248 (2008).
533 66. Bruner, K.M., *et al.* A quantitative approach for measuring the reservoir of latent HIV-1
534 proviruses. *Nature* **566**, 120-125 (2019).
535
536
537
538
539
540
541
542

543 **Table 1. OPHION Participant Characteristics**

Characteristic	Cohort		
	Non-Opioid	Opioid	Total*
Participants, N	12	24	36
Age			
Median (IQR†)	56 (50-61)	61 (55-65)	59 (54-65)
Sex			
Male N (%)	7 (58%)	17 (71%)	24 (67%)
Race			
Black N (%)	10 (83%)	6 (25%)	16 (44%)
White N (%)	2 (17%)	9 (38%)	11 (31%)
Hispanic/Latino** N (%)	0	2 (8%)	2 (6%)
American Indian N (%)	0	1 (4%)	1 (3%)
Declined/NA	0	6 (25%)	6 (17%)
Ethnicity			
Non-Hispanic N (%)	11 (92%)	13 (54%)	24 (67%)
Hispanic N (%)	1 (8%)	11 (46%)	12 (33%)
Duration of ART (months)			
Median (IQR)	162 (106-204)	136 (91-173)	144 (97-179)
Duration of viral suppression (months)			
Median (IQR)	69.5 (38-91)	79 (51-94)	75 (44-93)

544 *Percentage totals may not add up to 100 due to rounding. †IQR, interquartile range. **Participants may
545 identify as Hispanic/Latino either in response to a question about their race, or a follow-up question on
546 ethnicity. Participants who reported Hispanic ethnicity identified their race as either "White" or
547 "Declined/Not Available."

548

549

550

551

552

553 **Figure Legends**

554

555 **Figure 1.** HIV-1 reservoir size and intactness during opioid use. Quantifications were performed
556 on participants who used (n=24) or did not use (n=12) opioids. (a) HIV-1 persistence measures
557 in participants with (blue circles) and without (yellow circles) opioid use are shown. Data are
558 displayed on a logarithmic y-axis scale; DNA and RNA was extracted from 5 million PBMC.
559 Intact DNA was quantified with the IPDA assay. Mean values ± standard errors of the mean
560 (SEM) are shown. (b) 5' and 3' genomic deletions as a function of opioid use, mean values ±
561 95% CIs are displayed, (c) Opioid subgroup analysis. The reservoir size of intact, 5' deleted, and
562 3' deleted or hypermutated regions are shown. (d) The proportion of intact genomes as a function
563 of DNA copies and opioid use subgroup. Cohort 1, injection opioid use; cohort 2, prescribed oral
564 opioids for pain; cohort 3, methadone; cohort 4, suboxone; cohort 5, no opioid use.

565

566 **Figure 2.** HIV-1 latency reversal in OPHION participants. HIV-1 caRNA levels were quantified
567 after 24-hour incubations using 5 million PBMC and compared to a no-drug DMSO-containing
568 condition. Mean values and the 95% CIs are shown. (a) Combined data showing LRA responses
569 in thirty-six total participants with (blue circles) or without (yellow circles) opioid use. Data
570 from (a) was dichotomized by (b) opioid use, (c) sex (light purple circles, male; light grey
571 circles, female), and (d) race (light green circles, Black and American Indian; dark green circles,
572 white). (e) Opioid-use subgroup analysis highlighting LRA response to αCD3/αCD28 beads
573 from (a), as a function of opioid use subgroup. Means and SEM are shown. Dotted horizontal
574 line denotes a fold-change of 1. *$p<0.05$, ** $p<0.01$, *** $p<0.001$, and **** $p<0.0001$ for LRA
575 combinations, corrected for multiple comparisons. αCD3/αCD28, anti-CD3 anti-CD28

576 superparamagnetic beads; RMD, romidepsin; PNB, panobinostat; R, RMD 20nM; P, PNB
577 30nM; B, bryostatin 1nM; A, AZD5582 100nM.
578
579 **Figure 3.** Immune activation and cytokine induction during *ex vivo* LRA boosting. (a) Example
580 plots of $OX40^+PD\text{-}L1^+$, $OX40^+CD25^+$, and $CD69^+CD40L^+$ expression from live $CD4^+$ T cells in
581 PBMC samples incubated with DMSO control or an αCD3/αCD28 bead positive control for 18
582 hours, (b) Violin plots of surface activation-induced marker (AIM) response as a function of
583 LRA,. Results across three highly sensitive AIM assays for OPHION participants' samples
584 (n=36) are shown for comparison, (c) Quantification of LRA-induced surface CD69 expression
585 in live total $CD4^+$ T cells (n=36). Intracellular production of the cytokines TNF-α, IFN-γ, and IL-
586 2 during LRA exposure in (d) live $CD4^+$ and (e) $CD8^+$ T cells (n=36). Violin plot median values
587 are indicated by a solid black line; quartiles are shown with a dotted line. LRA conditions
588 without visible bars represent values < 0.1% of cells. *$p<0.05$, *** $p<0.001$, and **** $p<0.0001$
589 for LRA combinations, corrected for multiple comparisons. RMD, romidepsin; PNB,
590 panobinostat; R, RMD 20nM; P, PNB 30nM; B, bryostatin 1nM; A, AZD5582 100nM.
591
592 **Figure 4.** Histone H3 acetylation patterns during LRA exposure. (a) Violin plots showing the
593 proportion of live total $CD4^+$ T cells with acetylated histone H3, assessed by flow cytometry, (b)
594 Violin plot of mean fluorescence intensity (MFI) of acetylated histone H3 per live $CD4^+$ T cell.
595 Scatter plots of acetylated histone H3 levels per CD4 as a function of HIV-1 transcription in
596 response to (c) RMD and PNB monotherapy, (d) LRA boosting with HDACi and AZD5582, and
597 (e) HDACi in combination with low-dose bryostatin are shown. Acetylated histone levels and
598 HIV-1 reactivation with the combinations of HDACi and bryostatin were moderately positively

599 correlated (r=.25, p=.04). Violin plot median values are indicated by a solid black line; quartiles
600 are shown with a dotted line.
601
602 **Figure 5.** Comparative analysis of LRA boosting effects in PBMC and $CD4^+$ T cells.
603 Leukapheresis samples from HEAL cohort participants (n=11) were used to assess HIV-1
604 unspliced caRNA levels during (a) low-dose bryostatin-based and (b) AZD5582-based LRA
605 boosting combinations, when compared to PMA-ionomycin. Data are presented as means ±
606 SEM. Circle color is used to denote a given HEAL participant across Figure panels. (c) Absolute
607 HIV-1 unspliced caRNA levels in parallel PBMC and $CD4^+$ T cell LRA exposures. PBMC and
608 CD4 results are separated by a vertical dotted line. (d) Representation of the data in (c) as fold-
609 change in HIV-1 caRNA levels. (e) Corresponding HIV-1 RNA levels from culture supernatants.
610 (f) Multiply spliced HIV-1 RNA levels as determined in a modified TILDA assay, comparing
611 RMD-bryostatin combinations at two bryostatin concentrations to PMA-ionomycin. (g)
612 Combined OPHION and HEAL participant results (n=47) that summarize PBMC LRA boosting
613 responses, for LRA conditions common to both datasets. Results from OPHION participant
614 samples, carried over from Fig. 2a, are shown in grey circles. HEAL participant results are
615 shown in color. *p<0.05, ** p<0.01, *** p<0.001, **** p<0.0001, corrected for multiple
616 comparisons. NDC, no-drug control, contains 0.2% DMSO; PMAi, PMA with ionomycin; RMD,
617 romidepsin; PNB, panobinostat; R, RMD 20nM; P, PNB 30nM; B, bryostatin 1nM; A,
618 AZD5582 100nM.
619
620
621

622 **Supplementary Figures Legends**

623 **Supplementary Figure 1.** Substance use in the OPHION cohort. We assessed substance
624 use by (a) clinical urine toxicology testing and (b) self-reported substance use questionnaires.
625 Substance use results are separated by cohort groups by participant ID. Red squares indicate the
626 presence of that substance in a urine sample; unavailable data were marked with "X" in a gray
627 box. An expanded opiate panel was performed to assess for the presence of different opiate
628 formulations. Color squares in panel b reflect any reported use by participants in the last 30 days.
629 The numbers inside a given box indicate the number of days used this substance was reported to
630 be used in the last 30 days. Gradient of color from blue to red indicate increasing report of use
631 whereas white indicates no use. Concomitant use of alcohol, tobacco, marijuana, and gabapentin
632 in the OPHION cohort was common. *all fentanyl measures were confirmed by follow-on
633 quantification. Participants in the buprenorphine and methadone groups reported daily use of the
634 respective medication in the 30 days prior, whereas participants taking opioids for chronic pain
635 took opioids for 27-30 days in the 30 days preceding their enrollment in OPHION. 75% (N=3/4)
636 of active injection users had urine toxicology screens positive for cocaine corresponding with
637 self-report; all three reported smoking cocaine in the prior 30 days to specimen collection. One
638 of twelve participants in the methadone use group and 2/12 in the non-opiate use group also has
639 urine toxicology screens positive for cocaine. All active injection opioid users reported using
640 multiple drugs on the same day in the last 30 days compared to 1/12 participants in non-opioid
641 use group and 10/20 participants in methadone, buprenorphine and prescription opiate use
642 groups combined. N=3/4 active injection opioid users reported smoking marijuana in the last 30
643 days. 6 and 8 participants about the 12 participants in opioid use groups had urine toxicology
644 screens positive for benzodiazepines and gabapentin; all but 1 in both cases reported that this

645 substance was prescribed. No participant had urine toxicology screens positive for amphetamines
646 or barbiturates. All participants injecting opioids used tobacco in the preceding 30 days and,
647 overall, 23 of 36 OPHION participants used tobacco within the month prior to their blood
648 collection. 25% (N=6/24) of opioid use participants consumed alcohol in last 30 days compared
649 to 58% (7/12) in the control group.
650
651 **Supplementary Figure 2.** HIV-1 LRA boosting response in the OPHION cohort by ethnicity.
652 HIV-1 fold-increase in unspliced RNA transcription plotted as a function of self-reported
653 Hispanic (dark purple circles) or non-Hispanic (light blue circles) ethnicity.
654
655 **Supplementary Figure 3.** Flow cytometry gating strategies. Representative intracellular
656 cytokine staining plots for (a) control and (b) αCD3/αCD28 bead-exposed PBMC are shown. (c)
657 AIM assay and gating strategy and representative flow plots for control and αCD3/αCD28 bead-
658 exposed PBMC.
659
660 **Supplementary Figure 4.** LRA-induced immune activation as a function of opioid use. Results
661 obtained with the (a) OX40/PD-L1, (b) OX40/CD25, and (c) CD69/CD40L AIM assays are
662 reported for all ten conditions in the LRA panel, where samples from participants with (blue
663 circles) and without (yellow circles) opioid use are shown. Data are represented as means ± 95%
664 CIs. The highest measured levels in OX40/PDL1 assay with bryostatin 1nM, R+B, and P+B are
665 the same non-opioid-using participant. (d) Individual data points for $CD69^+$ live total $CD4^+$ T
666 cells, as a function of opioid use. (e) Comparative hierarchies of intracellular cytokine
667 production in $CD4^+$ and $CD8^+$ T cells exposed to αCD3/αCD28 beads. Data displayed in these

668 panels are identical to the data values shown in Main Fig. 3. *p<0.05, ** p<0.01, **** p<0.0001,
669 corrected for multiple comparisons. TNF, tumor necrosis factor-alpha; IFN, interferon-gamma;
670 IL-2, interleukin-2; CD4, $CD4^+$ T cells; CD8, $CD8^+$ T cells.
671
672 **Supplementary Figure 5.** Intracellular cytokine production, as a function of opioid use. Using
673 the same data displayed in Main Fig. 3, here we show individual data points, labelled as samples
674 from participants with (blue circles) and without (yellow circles) opioid use. $CD4^+$ T cell
675 production of (a) TNF-α, (b) IL-2, and (c) IFN-γ. CD8+ T cell production of (d) TNF-α, (e) IFN-
676 γ, (f) IL-2. No significant differences in cytokine production were observed by opioid use.
677
678 **Supplementary Figure 6.** Histone acetylation effects during LRA boosting, as a function of
679 opioid use. Using the same data displayed in Main Fig. 4, here we show individual data points,
680 labelled as samples from participants with (blue circles) and without (yellow circles) opioid use.
681 (a) The proportion of live total $CD4^+$ T cells with acetylated histone H3, assessed by flow
682 cytometry, (b) Mean fluorescence intensity (MFI) of acetylated histone H3 per live total $CD4^+$ T
683 cells.
684
685 **Supplementary Figure 7.** The effects of LRA boosting on human reference gene transcription.
686 Using leukapheresis samples from HEAL participants (n=9), we assessed and compared fold-
687 changes in transcription of three host genes: (a) IPO8, (b) TBP, and (c) UBE2D2. Reference
688 gene multiplexing was validated for (d) TBP and (e) UBE2D2 quantifications. The rationale to
689 study these three reference genes is as follows. IPO8 transcription is used as an internal control
690 by the AIDS Clinical Trials Group's Virology Specialty Laboratories to measure RNA integrity

691 in a dichotomous way. IPO8 Ct values >27 are used to suggest degradation of cellular samples in
692 storage, and samples with IPO8 Ct >27 do not report HIV-1 RNA values. Recent work by
693 Nancie Archin at the UNC HIV Cure Center identified TBP and UBE2D2 as two of the more
694 stable host genes during LRA exposures, which included PMA, AZD5582, and HDACi, among a
695 panel of eight LRA.
696
697 **Supplementary Figure 8.** Variance in LRA response. (a) Magnitude of HIV-1 caRNA
698 transcription fold-changes in biological replicate LRA experiments performed with HEAL
699 leukapheresis samples, derived from the data displayed in Main Fig 5a-c, (b) Box and whiskers
700 plot displaying the data of Fig. 5g as the mean (solid black horizontal line), inter-quartile range
701 (25th – 75th percentiles denoted as the borders of the vertical rectangle), and 5th-95th percentiles
702 (whiskers, error bars). Values below and above the whiskers are shown as individual data points.
703 PMA-iono, PMA with ionomycin; RMD, romidepsin; PNB, panobinostat; R, RMD 20nM; P,
704 PNB 30nM; B, bryostatin 1nM; A, AZD5582 100nM.
705
706 **Supplementary Tables**
707 **Supplementary Table 1** – Breakdown of OPHION cohort into opioid use subgroups
708 **Supplementary Table 2** – HEAL Participant Characteristics
709
710
711
712
713

714 **Online Methods**

715 **Study Design and Clinical Cohorts**

716 The Opioids, HIV, and Translation (OPHION) study is a prospective cohort study of participants
717 living with HIV on suppressive antiretroviral therapy recruited from Boston Medical Center
718 which serves one of the largest populations of people living with HIV (PLWH) in Massachusetts,
719 including a disproportionately large number of persons with opioid and substance use disorders.
720 Eligible PLWH were required to currently be on antiretroviral therapy and virologically
721 suppressed (defined as undetectable plasma HIV-1 RNA or <20 copies/ml) for a minimum of 12
722 months prior to enrollment. Individuals were recruited into 1 of 5 cohorts: (1) active injection
723 opioid use, defined as self-report on injecting opioids at least once per week, (2) Methadone
724 maintenance therapy for at least 3 months, (3) buprenorphine-naloxone therapy for at least 3
725 months, (4) Prescription oral opioid use for at least 6 months or (5) No opioid use within the past
726 1 year representing a control cohort. Eligibility into each of the five cohorts was confirmed with
727 a urine toxicology performed at the BMC central laboratory, which includes evaluation for urine
728 drug metabolites including opiates and non-opioid substances as well as an expanded opioid
729 panel which included fentanyl or norfentanyl metabolites. Exclusionary criteria included ongoing
730 immunosuppression and pregnancy; patients who reported injecting non-opioid substances were
731 also not eligible. Once consented and enrolled, each participant underwent blood collection for
732 same day PBMC extraction as well as urine collection for gabapentin and benzodiazepine
733 metabolites. Participants also completed an extensive survey on their current and prior substance
734 use (including alcohol and tobacco use) based the addiction severity index (ASI) [63] and Texas
735 Christian University (TCU) drug screen [64]. HIV and other clinical information including ART

736 treatment history, duration of virologic suppression and comorbidity status including hepatitis C
737 and B were abstracted from the medical record.
738 The HIV Eradication and Latency (HEAL) Cohort is a longitudinal biorepository study of
739 participants with HIV. Inclusion criteria for HEAL participants in this study were 1) ART-treated
740 participants with HIV-1 who were virologically suppressed, defined as plasma HIV-1 RNA less
741 than assay (most commonly less than 20 copies/mL, without blips) for >1 year and 2) had
742 sufficient available amounts of cryopreserved PBMC for the proposed analyses. These cohort
743 studies are performed in accordance with the principles of the Declaration of Helsinki. The
744 institutional review boards at Boston Medical Center and Brigham and Women's Hospital (Mass
745 General Brigham Human Research Committee) approved the study protocols. Written informed
746 consent was obtained from all participants. Experimenters were blinded to all clinical data and to
747 OPHION subgroup assignments.
748
749 **Quantification of HIV-1 persistence markers**
750 Genomic DNA and total RNA were isolated from approximately $5x10^6$ peripheral blood
751 mononuclear cells (PBMC) or total $CD4^+$ T cells (AllPrep DNA/RNA kit, Qiagen). Total HIV-1
752 DNA and unspliced cell-associated RNA (caRNA) levels were quantified in triplicate by real-
753 time PCR as previously described, modified to include Taqman Universal Mastermix (DNA) or
754 Taqman Fast Virus 1-Step Mastermix (RNA) [65]. HIV-1 quantifications used forward primer 5'-
755 TACTGACGCTCTCGCACC-3', reverse primer 5'-TCTCGACGCAGGACTCG-3', and probe
756 5' FAM-CTCTCTCCTTCTAGCCTC-MGB 3' (ThermoFisher Scientific). DNA cycling
757 conditions in a total reaction volume of 25µL were 95°C for 15 min followed by 40 cycles of
758 95°C for 15 sec and 60°C for 1 min. RNA cycling conditions in a total reaction volume of 20µL

759 were 55°C for 15 min, 95°C for 20 sec, followed by 40 cycles of 95°C for 3 sec and 60°C for 30
760 sec. Approximately 500ng of genomic DNA were assessed per well. The limits of quantification
761 for total HIV-1 DNA and unspliced caRNA were 1 and 3 copies per reaction, respectively.
762 Limits of detection were calculated per timepoint and participant sample, considering the
763 average number of copies detected across triplicate measurements. Cell input numbers were
764 quantified by human genome equivalents of CCR5 DNA using forward primer 5'-
765 ATGATTCCTGGGAGAGACGC-3', reverse primer 5'-AGCCAGGACGGTCACCTT-3', and
766 probe 5' FAM-CTCTCTCCTTCTAGCCTC-MGB 3' (ThermoFisher Scientific) as described [65].
767

768 **Intact proviral DNA assay**

769 HIV-1 DNA from isolated PBMC DNA was measured using the intact proviral DNA assay
770 (IPDA) [66]. Briefly, a multiplex droplet digital PCR assay was performed using primer and probe
771 sets targeting the Psi packaging signal and env regions of the HIV-1 genome using 700 ng DNA
772 per well. Intact provirus genomes were indicated in double positive droplets whereas incomplete
773 genomes were single positive and classified as either 5' (Psi-/env+) or 3' (Psi+/env-) deletions.
774 Quantified proviral sequences were normalized to cell number reference gene RPP30 and
775 expressed as copies per million PBMC. Data was generated using the Bio-Rad QX200 Droplet
776 Digital PCR system and analyzed using QuantaSoft Data Analysis Software.
777

778 **Multiply spliced HIV-1 transcripts**

779 To measure the frequency of total $CD4^+$ T cells with inducible multiply spliced HIV-1 RNA, we
780 performed the TILDA assay, as previously described, with two modifications [46]. First, to reduce
781 the 95% CIs around our frequency estimates, we used 36 x 10^6 cells/mL as our first dilution,

782 rather than the 18 x 10^6 cells/mL used in Procopio, et al. Second, to harmonize our PMA-
783 ionomycin concentrations with LRA experiments, we reduced the PMA concentration from its
784 original 100 ng/mL to 50ng/mL in our TILDA assays. The duration of virologic suppression in
785 our HEAL participants was similar to previously reported participants [46].
786
787 **Reference gene quantification**
788 Extracted PBMC RNA was used to quantify transcription levels of three host genes, IPO8, TBP,
789 and UBE2D2, typically immediately after the loading of HIV-1 caRNA qPCR plates was
790 complete. IPO8 quantifications used forward primer 5'- CCTTTGTACAACAGAAGGCAC -3',
791 reverse primer 5'- TGCACGTCTCAGGTTTTTGC -3', and probe 5' FAM-
792 TCCGCATAAATCCATTGATTCTGC -MGB 3' (ThermoFisher Scientific); TBP
793 quantifications used forward primer 5'- CAGTGAATCTTGGTTGTAAACTTGA -3', reverse
794 primer 5'- TCGTGGCTCTCTTATCCTCAT -3', and probe 5' FAM-
795 CGCAGCAAACCGCTTGGGATTAT -MGB 3' (ThermoFisher Scientific); and UBE2D2
796 quantifications used forward primer 5'- GTACTCTTGTCCATCTGTTCTCTG -3', reverse
797 primer 5'- CCATTCCCGAGCTATTCTGTT -3', and probe 5' VIC-
798 CCGAGCAATCTCAGGCACTAAAGGA -MGB 3' (ThermoFisher Scientific). To generate
799 IPO8 standards, we cloned a fragment corresponding to nucleotides 3636-3707 of IPO8 mRNA
800 (Sequence ID NM_006390.4) into a pCR4-TOPO vector (ThermoFisher Scientific, Cat. No.
801 K458001). To generate TBP standards, a fragment corresponding to nucleotides 649-1037 of
802 TBP mRNA (Sequence ID NM_003194) was cloned into a pCR4-TOPO vector. To generate
803 UBE2D2 standards, a fragment corresponding to nucleotides 729-1164 of UBE2D2 mRNA
804 (Sequence ID NM_181838.2) was cloned into a pCR4-TOPO vector. Reference gene RNA was

805 synthesized using T3 Megascript Kit (ThermoFisher Cat. No. AM1333 and cleaned (RNease
806 MinElute Cleanup Kit, Qiagen, Cat. No. 74204) before serially diluting across a range of 10^6 –
807 10^3 copies per well. After TBP and UBE2D2 standards were individually validated, TBP (T)
808 and UBE2D2 (U) RNA were diluted separately and aliquoted together as one set of multiplex
809 standards. T and U standards were validated to demonstrate overlap of individual and
810 multiplexed standards curves. The assay was optimized to run all host gene standards and
811 samples on one 96-well reaction plate in a total reaction volume of 20µL using cycling
812 conditions of 55°C for 5 min, 95°C for 20 sec, followed by 40 cycles of 95°C for 3 sec and 56°C
813 for 30 sec. Reference gene standards and samples were run in duplicate. IPO8, TBP, and
814 UBE2D2 RNA copies per million PBMC were calculated by dividing copies per total sample by
815 number of cells per sample, determined by CCR5 quantification, and normalized to $1x10^6$ cells.
816 Fold changes were calculated by dividing the RNA copy number obtained per million PBMC for
817 each LRA condition by the 0.2% DMSO control condition's reference gene RNA copies/million
818 PBMC.
819

820 **HIV-1 latency reversal**

821 OPHION and HEAL participant peripheral blood mononuclear cells (PBMC) were isolated from
822 large volume (90 – 180cc) peripheral blood or leukapheresis collections by density centrifugation
823 and cryopreserved. Cryopreserved PBMC were thawed, pelleted, and transferred to RPMI media
824 supplemented with 10% fetal bovine serum, 2 µM raltegravir, and 2 µM tenofovir (R10 +
825 TDF/RAL) at a concentration of $1x10^6$ cells/mL. Cells were rested in a humidified CO_2
826 incubator at 37°C for three hours (hrs). After 3hrs, cells were counted and assessed for viability.
827 For $CD4^+$ T cell experiments, PBMC were pelleted, resuspended in EasySep Buffer (StemCell

828 Technologies, cat. no. 20144), and isolated with EasySep Human $CD4^+$ T Cell Enrichment Kit
829 (StemCell cat. no. 19052) per the manufacturer's instructions. A total of $5x10^6$ PBMC, or total
830 $CD4^+$ T cells, were aliquoted into 5mL of fresh R10 + RAL/TDF in 6-well sterile cell culture
831 plates. Cells were incubated in the presence or absence of the following LRA conditions: 0.2%
832 DMSO, 1:1 αCD3/αCD28 beads (Life Technologies, cat. no. 11131D) to cells with 30 U/mL IL-
833 2 (R&D Systems, cat. no. 202-IL-500), romidepsin 20 nM (Sigma , cat. no. SML1175),
834 panobinostat 30nM (Sigma, cat. no. SML3060), bryostatin-1 1nM (Sigma, cat. no. B7431),
835 AZD5582 100nM (ChemieTek, cat. no. CT-A5582), romidepsin 20 nM plus bryostatin-1 1nM,
836 panobinostat 30nM plus bryostatin-1 1nM 100nM, romidepsin 20 nM plus AZD5582 100nM,
837 panobinostat 30nM plus AZD5582 100nM, and phorbol 12-myristate 13-acetate (PMA)
838 50ng/mL (Sigma, cat. no. P1585) in combination with ionomycin 1μM (Sigma, cat. no. I9657).
839 To provide a known positive control for subsequent immunology assessments, αCD3/αCD28
840 beads were used with OPHION samples. Cultures were incubated at 37°C for 24 hours. After 24
841 hours, cells were prepared for nucleic acid extractions.
842
843 **Activation Induced Marker (AIM) assay**
844 AIM assays were performed as previously described [43]. Briefly, cryopreserved PBMC were
845 thawed, washed, resuspended in R10, and rested for 3 hours at 37°C. Following the 3-hour rest
846 interval, the appropriate number of cells were transferred to a 48-well plate and subsequently
847 treated with CD40 blocking antibody (Miltenyi Biotec, cat. no. 130-094-133) for a final
848 concentration of 0.5ug/mL for 15 minutes at 37°C. Cells were incubated in the presence or
849 absence of our 10-LRA panel, as previously described. After an 18hr incubation, cells were
850 harvested and stained for 50 minutes at 4°C with the surface staining monoclonal antibodies

851 (mAb); (PD-L1-PE/Cy7 (Biolegend, cat. no. 329717), CD40L-PE (BD Biosciences [BD], cat.
852 no. 561720), OX40-APC (BD cat. no. 563473), CD69-BV650 (Biolegend cat. no. 310933),
853 CD3-BV605 (Biolegend cat. no. 317322), CD4-BV421 (BD cat. no. 562424), CD8-PerCp-Cy5.5
854 (BD cat. no. 560662), CD25- BUV395 (BD cat. no. 564034) and LIVE/DEAD Near-IR stain
855 (ThermoFisher cat. no. L34975), washed, fixed and permeabilized (BD cytofix fixation buffer,
856 cat. no. 554655), and then stained for 30 minutes at 4°C with intracellular mAb Acetyl-histone
857 H3-Alexa Fluor 488 (Cell Signaling Technology, cat. no. 9683S) in 1x perm/wash buffer (BD,
858 cat. no. 554723). The cells were washed and fixed (BD cytofix fixation buffer, cat. no. 554655)
859 prior to flow cytometry analysis.
860
861 **Intracellular cytokine staining**
862 Cryopreserved PBMC were thawed, washed, resuspended in RPMI + 10% FBS (R10), and
863 rested for 3 hours at 37°C. Following the 3-hour rest interval, the appropriate number of cells
864 were transferred to a 48-well plate and incubated for 2 hrs with our panel of 10 LRA. Following
865 this 2-hour incubation period, GolgiPlug (BD, cat. no. 555029) and GolgiStop (BD, cat. no.
866 554724) were added to each condition at a concentration of 1:1000 and 6:10000 respectively,
867 then incubated at 37°C for an additional 16 hrs. Cells were harvested, pelleted, resuspended,
868 stained for 20 minutes at 4°C with surface staining mAb (CD3-BV605, CD4-BV421, CD8-
869 PerCp-Cy5.5 and LIVE/DEAD Near-IR stain), fixed and permeabilized as described above, and
870 then stained for 30 minutes at 4°C with the intracellular mAb TNF-α- PE/Dazzle-594 (Biolegend
871 cat. no. 502946), IL-2- PE/Cy7 (BD cat. no. 560707) and IFN-γ- BV510 (Biolegend cat. no.
872 502544). PBMC were washed and fixed in (BD cytofix fixation buffer, cat. no. 554655) prior to
873 flow cytometry analysis, as described above.

874

875 **Flow cytometry**

876 Cells were acquired on a BD LSRFortessa using FACSDiva. Analysis was performed using
877 FlowJo software versions 10.6.2 (Treestar, Versions 10 for Mac). Representative gating
878 strategies can be found in the supplemental figures.

879

880 **Statistical analysis**

881 Statistical analyses were performed using GraphPad Prism 9 for macOS. Means, medians, 95%
882 confidence intervals, and standard errors of the mean were calculated. The pre-specified primary
883 outcome of OPHION was a comparison of $\log_{10}$ PBMC HIV-1 caRNA levels between
884 participants who use and do not use opioids. The pre-specified outcome for OPHION latency
885 reversal experiments was the difference in HIV-1 caRNA levels between LRA treatment groups
886 and across opioid use groups. To assess for changes in HIV-1 caRNA, we performed Kruskal-
887 Wallis testing of all participants together for each of the LRAs with Dunn's multiple comparison
888 test, comparing the mean rank of each LRA condition with the mean rank of every other LRA
889 condition. An identical approach was taken with a series of exploratory analyses with OPHION
890 participant samples that assessed histone acetylation, surface activation, and intracellular
891 cytokine production, and with the exploratory statistical analyses performed on experiments with
892 HEAL participant samples.

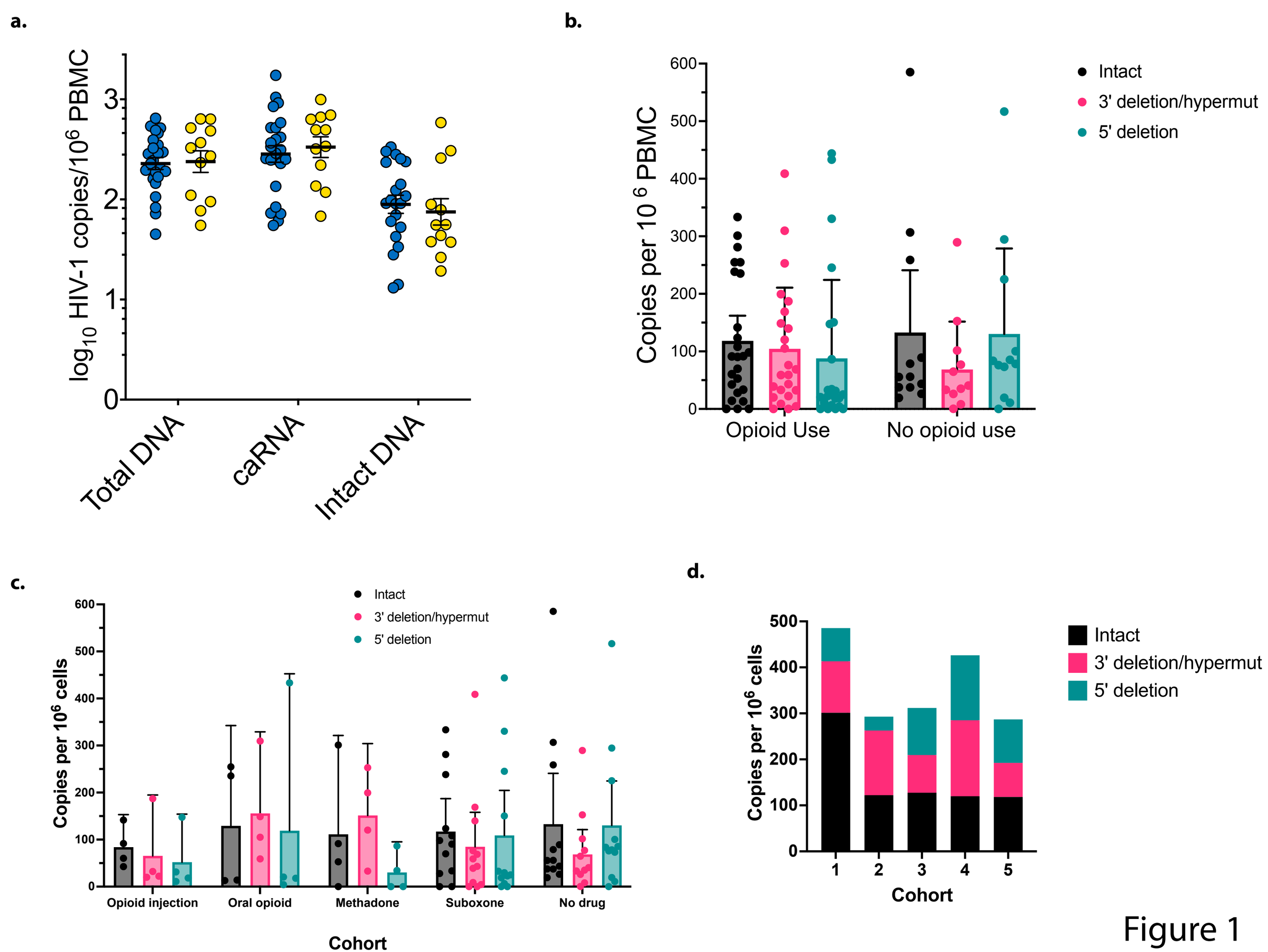
a.
log10 HIV-1 copies/10^6 PBMC
0
1
2
3
Total DNA
caRNA
Intact DNA
b.
Copies per 10^6 PBMC
0
100
200
300
400
500
600
Opioid Use
No opioid use
Intact
3' deletion/hypermut
5' deletion
c.
Copies per 10^6 cells
0
100
200
300
400
500
600
Opioid injection
Oral opioid
Methadone
Suboxone
No drug
Cohort
Intact
3' deletion/hypermut
5' deletion
d.
Copies per 10^6 cells
0
100
200
300
400
500
1
2
3
4
5
Cohort
Intact
3' deletion/hypermut
5' deletion

Figure 1

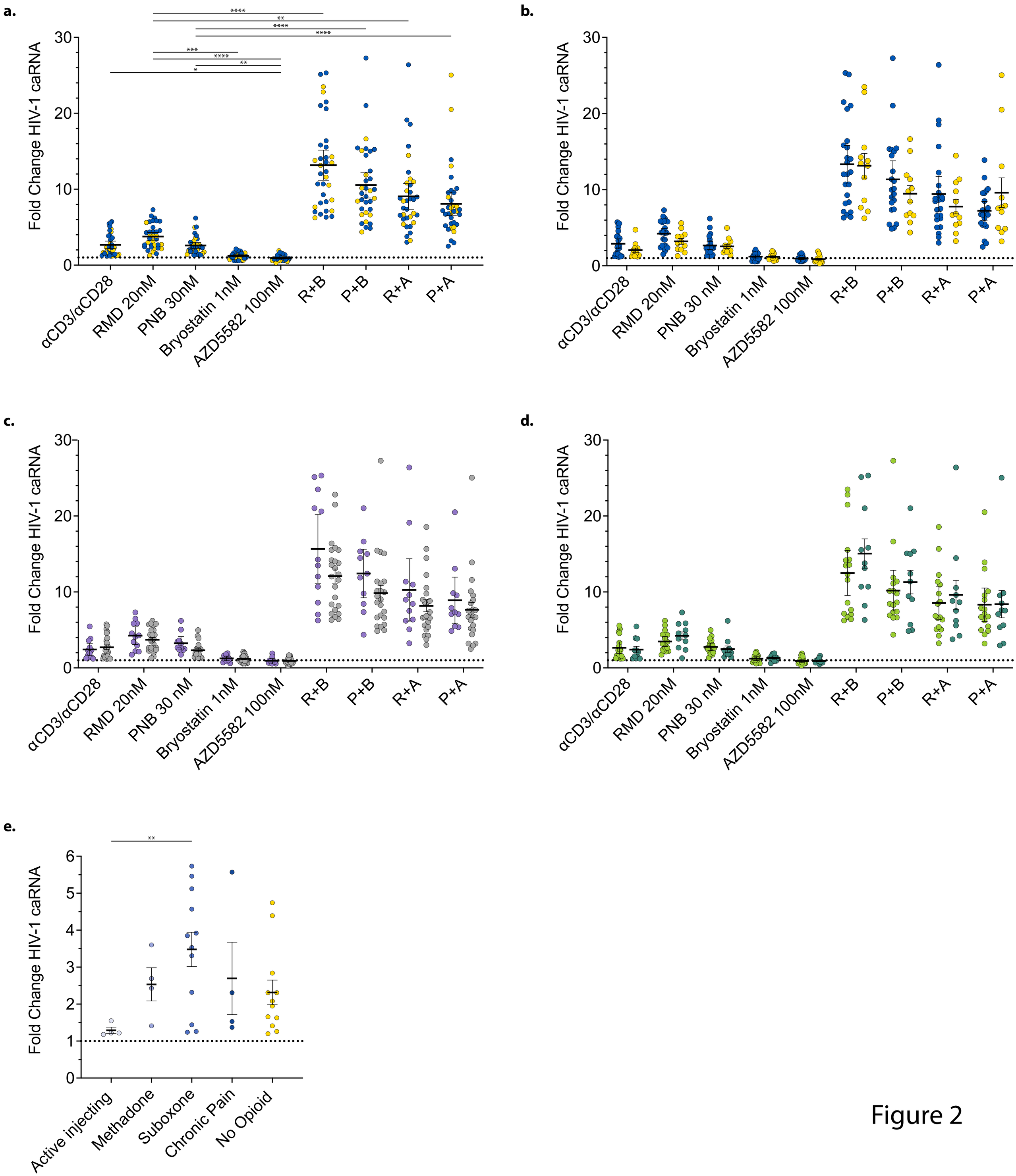
a.
b.
c.
d.
e.
Fold Change HIV-1 caRNA
αCD3/αCD28
RMD 20nM
PNB 30nM
PNB 30 nM
Bryostatin 1nM
AZD5582 100nM
R+B
P+B
R+A
P+A
Active injecting
Methadone
Suboxone
Chronic Pain
No Opioid

Figure 2

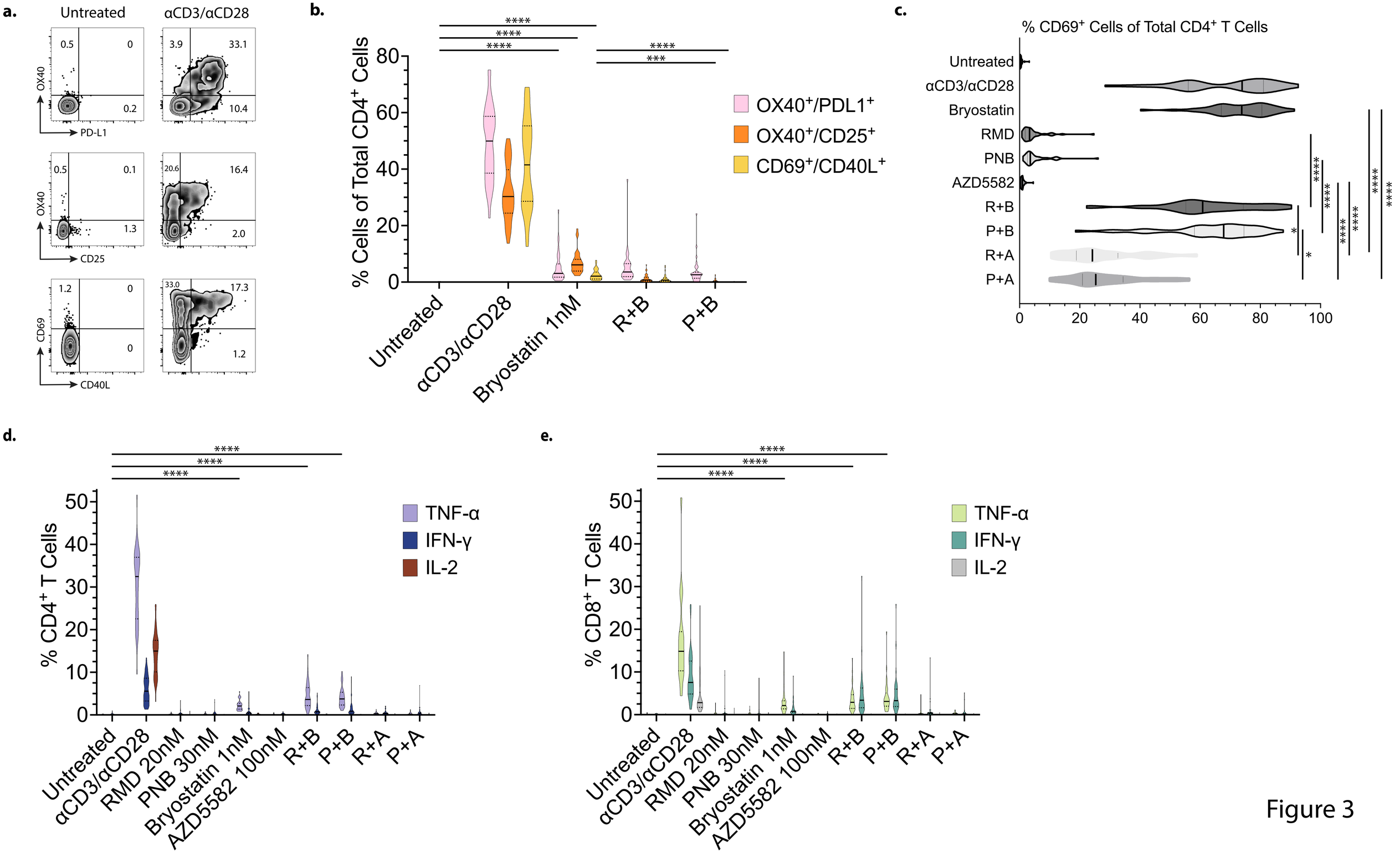
a.
Untreated
αCD3/αCD28
OX40
PD-L1
CD25
CD69
CD40L
b.
% Cells of Total CD4+ Cells
OX40+/PDL1+
OX40+/CD25+
CD69+/CD40L+
Untreated
αCD3/αCD28
Bryostatin 1nM
R+B
P+B
c.
% CD69+ Cells of Total CD4+ T Cells
Untreated
αCD3/αCD28
Bryostatin
RMD
PNB
AZD5582
R+B
P+B
R+A
P+A
d.
% CD4+ T Cells
TNF-α
IFN-γ
IL-2
Untreated
αCD3/αCD28
RMD 20nM
PNB 30nM
Bryostatin 1nM
AZD5582 100nM
R+B
P+B
R+A
P+A
e.
% CD8+ T Cells
TNF-α
IFN-γ
IL-2
Untreated
αCD3/αCD28
RMD 20nM
PNB 30nM
Bryostatin 1nM
AZD5582 100nM
R+B
P+B
R+A
P+A

Figure 3

Figure 4

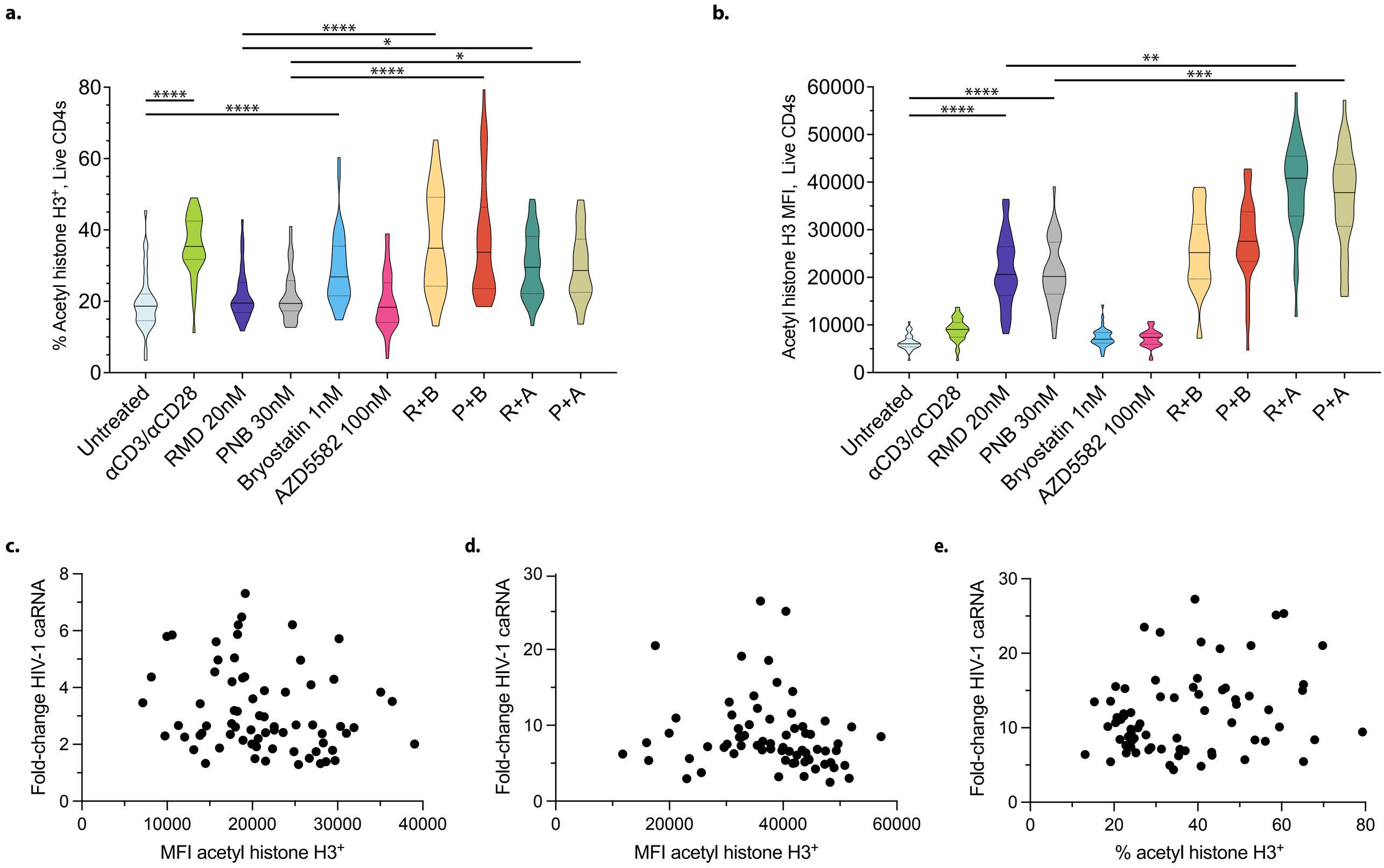
a.
% Acetyl histone H3+, Live CD4s
0
20
40
60
80
****
****
****
*
*
****
Untreated
αCD3/αCD28
RMD 20nM
PNB 30nM
Bryostatin 1nM
AZD5582 100nM
R+B
P+B
R+A
P+A
b.
Acetyl histone H3 MFI, Live CD4s
0
10000
20000
30000
40000
50000
60000
****
****
**
***
Untreated
αCD3/αCD28
RMD 20nM
PNB 30nM
Bryostatin 1nM
AZD5582 100nM
R+B
P+B
R+A
P+A
c.
Fold-change HIV-1 caRNA
MFI acetyl histone H3+
d.
Fold-change HIV-1 caRNA
MFI acetyl histone H3+
e.
Fold-change HIV-1 caRNA
% acetyl histone H3+

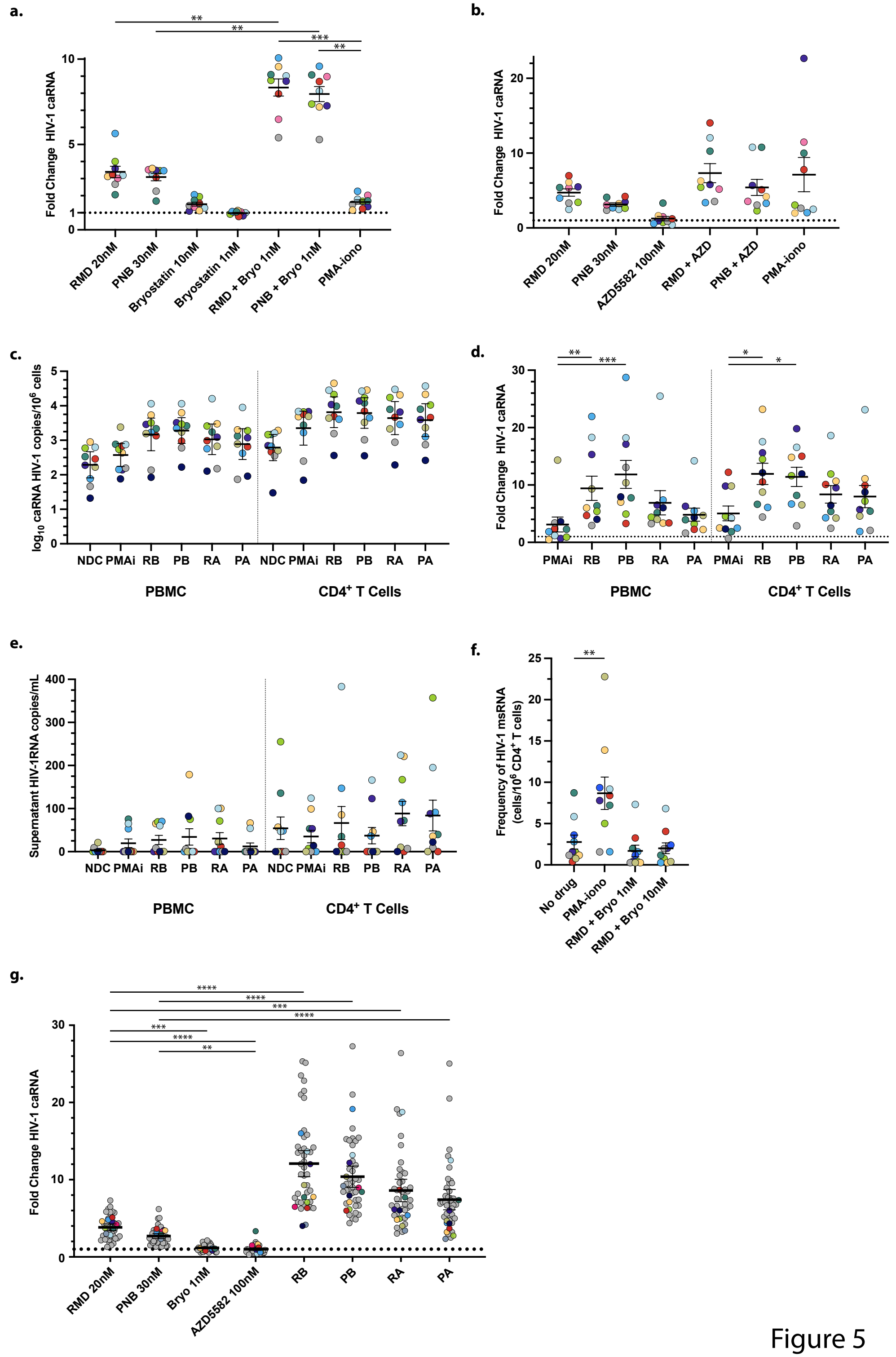
a.
Fold Change HIV-1 caRNA
RMD 20nM
PNB 30nM
Bryostatin 10nM
Bryostatin 1nM
RMD + Bryo 1nM
PNB + Bryo 1nM
PMA-iono
b.
Fold Change HIV-1 caRNA
RMD 20nM
PNB 30nM
AZD5582 100nM
RMD + AZD
PNB + AZD
PMA-iono
c.
log10 caRNA HIV-1 copies/10^6 cells
NDC PMAi RB PB RA PA NDC PMAi RB PB RA PA
PBMC
CD4+ T Cells
d.
Fold Change HIV-1 caRNA
PMAi RB PB RA PA PMAi RB PB RA PA
PBMC
CD4+ T Cells
e.
Supernatant HIV-1RNA copies/mL
NDC PMAi RB PB RA PA NDC PMAi RB PB RA PA
PBMC
CD4+ T Cells
f.
Frequency of HIV-1 msRNA (cells/10^6 CD4+ T cells)
No drug
PMA-iono
RMD + Bryo 1nM
RMD + Bryo 10nM
g.
Fold Change HIV-1 caRNA
RMD 20nM
PNB 30nM
Bryo 1nM
AZD5582 100nM
RB
PB
RA
PA

Figure 5